

# Hybrid Core–Shell Nanowire Forests as Self-Selective Chemical Connectors

Hyunhyub Ko,<sup>†,‡,§,||</sup> Jongho Lee,<sup>†,⊥</sup> Bryan E. Schubert,<sup>†,‡</sup> Yu-Lun Chueh,<sup>‡,§,||</sup>  
Paul W. Leu,<sup>‡,§,||</sup> Ronald S. Fearing,<sup>\*,‡</sup> and Ali Javey<sup>\*,‡,§,||</sup>

Department of Electrical Engineering and Computer Sciences, University of California at Berkeley, Berkeley, California 94720, Materials Sciences Division, Lawrence Berkeley National Laboratory, Berkeley, California 94720, Berkeley Sensor and Actuator Center, University of California at Berkeley, Berkeley, California 94720, and Department of Mechanical Engineering, University of California at Berkeley, Berkeley, California 94720

Received February 2, 2009; Revised Manuscript Received March 15, 2009

## ABSTRACT

Conventional connectors utilize mechanical, magnetic, or electrostatic interactions to enable highly specific and reversible binding of the components (i.e., mates) for a wide range of applications. As the connectors are miniaturized to small scales, a number of shortcomings, including low binding strength, high engagement/disengagement energies, difficulties with the engagement, fabrication challenges, and the lack of reliability are presented that limit their successful operation. Here, we report unisex, *chemical* connectors based on hybrid, inorganic/organic nanowire (NW) forests that utilize weak van der Waals bonding that is amplified by the high aspect ratio geometric configuration of the NWs to enable highly specific and versatile binding of the components. Uniquely, NW *chemical* connectors exhibit high macroscopic shear adhesion strength ( $\sim 163$  N/cm<sup>2</sup>) with minimal binding to non-self-similar surfaces, anisotropic adhesion behavior (shear to normal strength ratio  $\sim 25$ ), reusability ( $\sim 27$  attach/detach cycles), and efficient binding for both micro- and macroscale dimensions.

At millimeter dimensions or less, the conventional mechanical, electrostatic, and magnetic connectors<sup>1,2</sup> suffer from severe performance and reliability degradation that presents a major challenge for applications that require specific binding of miniaturized components.<sup>3,4</sup> Therefore, there is a major need for a new connector concept that perhaps operates with a different binding principle. In contrast to the conventional connectors (e.g., buttons, zippers, and Velcro), universal adhesives (e.g., tapes, glues, and synthetic gecko adhesives)<sup>5–10</sup> enable efficient binding even for miniaturized components as they utilize chemical binding interactions which maintain their binding ability with size reduction. A challenge in using chemical binding interactions<sup>11–14</sup> for connector applications arises in the need for reversible and specific, rather than permanent and universal binding between the components. For instance, while van der Waals (vdW) interactions are reversible, they are highly nonspecific which enables the gecko adhesives to bind efficiently to various

surfaces with ease<sup>5–11</sup>—a nonideal property for connectors. To address the need for a new connector technology, here we report *chemical* connectors that utilize reversible vdW bonding interactions of hybrid inorganic/organic NW forests. The weak vdW bond strengths result in the low adhesion of the relatively stiff, hybrid NWs on non-self-similar surfaces, in distinct contrast to nanotube or polymeric-based synthetic gecko adhesive which utilize materials with lower stiffness. However, high shear adhesion is obtained once the hybrid NW forests are engaged with self-similar surfaces due to the drastic amplification of the contact area arising from the interpenetration of the high-aspect ratio NWs. As a result, highly specific and versatile *chemical* connectors with unique properties are enabled that exhibit tunable properties through composition control of the hybrid NW components.

In this study, Ge NW forests (diameter,  $d = 20\text{--}30$  nm and length,  $L \sim 30$   $\mu\text{m}$ ) were utilized as the backbone of the *chemical* connectors (Figure 1a) to enable nanofibrillar structures with high aspect ratios (see Methods). Cross-sectional and top-view scanning electron microscopy (SEM) images (Figure 1b,c) of the Ge NW arrays indicate that most of the NWs are grown vertically on the substrate but with random orientation, resembling a forest. Clearly, the grown NWs sustain their high aspect ratio without aggregation or collapse (Figure 1b,c), in part due to the high Young's

\* Corresponding authors: ajavey@eecs.berkeley.edu, ronf@eecs.berkeley.edu.

<sup>†</sup> These authors contributed equally.

<sup>‡</sup> Department of Electrical Engineering and Computer Sciences, University of California at Berkeley.

<sup>§</sup> Materials Sciences Division, Lawrence Berkeley National Laboratory.

<sup>||</sup> Berkeley Sensor and Actuator Center, University of California at Berkeley.

<sup>⊥</sup> Department of Mechanical Engineering, University of California at Berkeley.

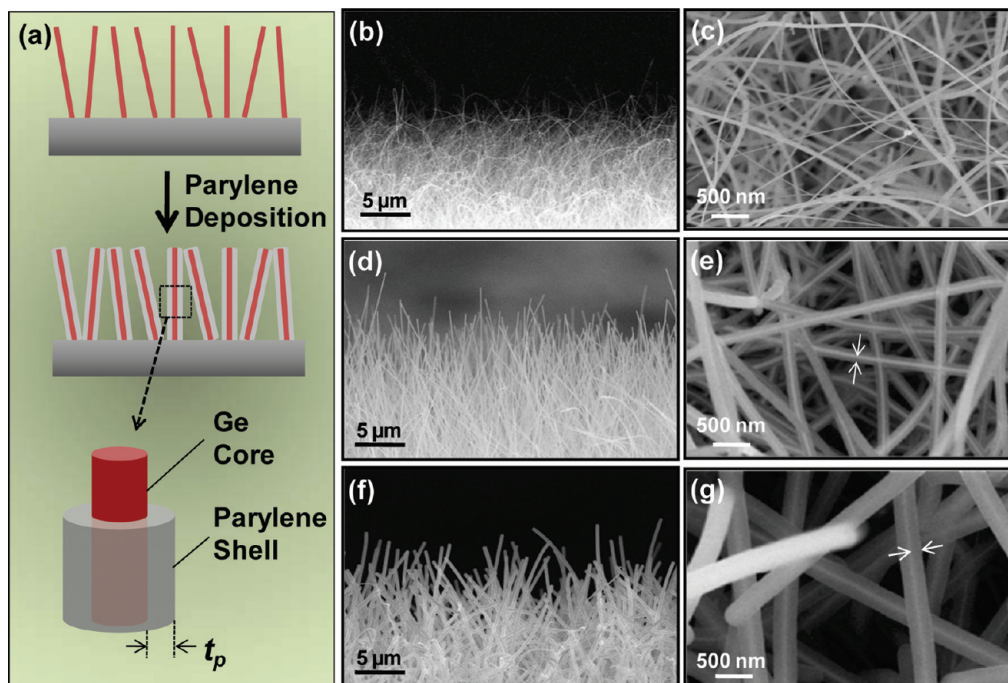


**Figure 1.** Ge/parylene core/shell hybrid NW forests for unisex, *chemical* connectors. (a) Schematic of the fabrication procedure for the core–shell NW forests. Cross sectional and top-view SEM images of Ge NWs (b, c) without parylene coating, (d, e) with 50 nm parylene coating, and (f, g) with 200 nm parylene coating, respectively. The white arrows in (e, g) indicate the parylene shell.

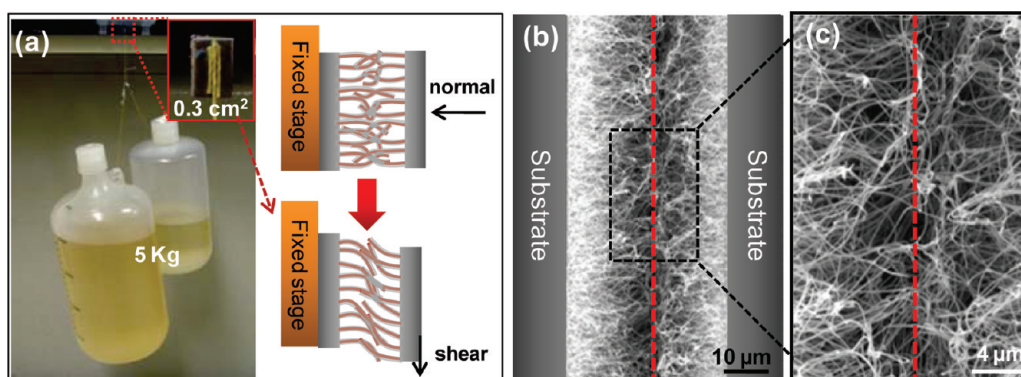


**Figure 2.** NW connectors in the engaged mode. (a) 5 kg of weight is suspended from a vertical surface by the use of NW connectors with a  $\sim 30 \text{ mm}^2$  area. The schematic shows the interpenetrated NWs under a normal (top) and shear force (bottom). (b, c) Cross-sectional SEM images of the engaged NW connectors.

modulus ( $\sim 100\text{--}150 \text{ GPa}$ )<sup>15</sup> of the Ge NWs. Next, a thin parylene layer with a thickness  $t_p = 10\text{--}400 \text{ nm}$  was deposited in the gas phase, resulting in free-standing Ge/parylene core/shell NW arrays (Figure 1). The parylene coating was highly uniform (Figure 1) with minimal NW surface roughness as evident from transmission electron microscopy (TEM) analyses (see Figure S1 in Supporting Information). The parylene shell has three important functions. First, the compliance of the polymeric shells provides an intimate contact with the opposite surface, therefore increasing the vdW interactions in the engaged mode.<sup>16</sup> Second, the viscoelastic property of parylene prevents the brittle failure of NW arrays<sup>17</sup> and thus reinforces the mechanical robustness and reusability of the NW connectors. Finally, parylene is an ideal passivation material with superb chemical properties, including low permeability to most gases

and water vapor, high chemical resistivity, and hydrophobic surface properties.<sup>18</sup>

The performance of the NW connectors was evaluated by macroscopic shear adhesion tests (Figure 2). An example of the strong binding achieved is shown in Figure 2a in which a hand-engaged NW connector with a surface area of  $\sim 0.5 \times 0.6 \text{ cm}^2$  enables 5 kg ( $\sim 49 \text{ N}$ ) of weight to be hung from a vertical surface without failure. This adhesion ability corresponds to a shear adhesion strength of  $\sim 163 \text{ N/cm}^2$ , well above the shear adhesion strengths obtainable by most connector technologies (Velcro  $5\text{--}15 \text{ N/cm}^2$ )<sup>19</sup> and comparable or better than those achieved with universal adhesives (carbon nanotube gecko adhesives  $\sim 100 \text{ N/cm}^2$ ).<sup>20</sup> The strong shear binding arises from the large contact area between the interpenetrating NWs, effectively amplifying the vdW interactions.

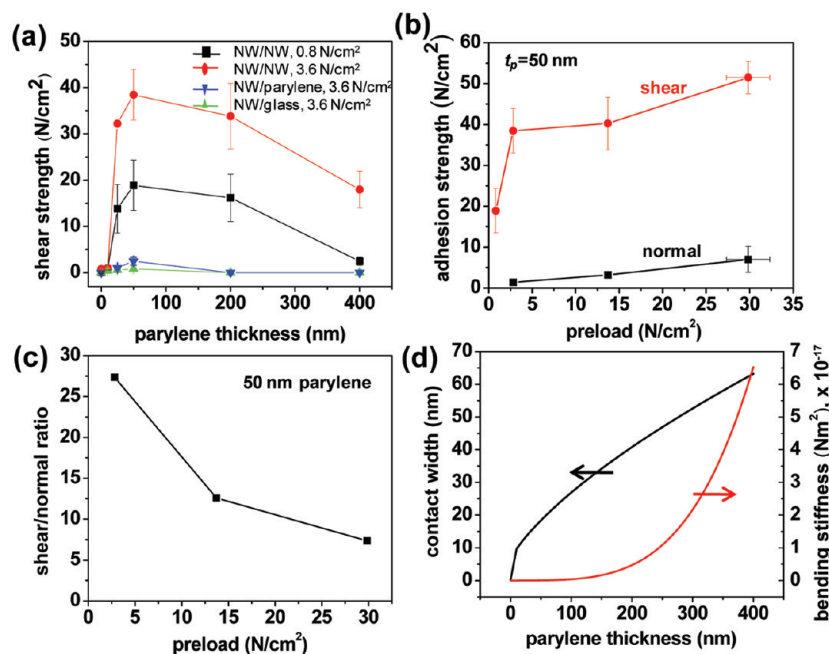


**Figure 3.** Adhesion characteristics of the NW connectors. (a) Shear strength of NW connectors as a function of the parylene shell thickness for normal preload forces of 0.8 and 3.6 N/cm<sup>2</sup>. For comparison purposes, the shear strength of NW forests on glass (green curve) and parylene coated glass (blue curve) surfaces is also shown. (b) Shear and normal strength for  $t_p = 50$  nm as a function of the normal preload. (c) Shear to normal strength ratio as a function of the preload, showing the anisotropic adhesion behavior of NW connectors. (d) The calculated contact width between two NWs overlapped by 5  $\mu\text{m}$  under a normal force of 200 nN (black curve) and the bending stiffness of a single NW (red curve) as a function of the parylene shell thickness.

To further characterize the properties of NW connectors and shed light on their binding mechanism, we systematically measured the macroscopic shear adhesion strength as a function of the parylene shell thickness (Figure 3a). The measurements were conducted by first engaging the connectors (area  $\sim 0.3$  cm<sup>2</sup>) with a normal preload force. The preload force was then removed while a continuously increasing shear force was applied until a failure (i.e., detachment) was observed. The force at failure corresponds to the maximum shear strength of the connectors. As depicted in Figure 3a, the shear adhesion properties strongly depend on the thickness of the polymeric shell and the applied preload force. Specifically, a weak shear strength of  $\sim 0.8$  N/cm<sup>2</sup> is attained for the pristine GeNWs (i.e., without a parylene shell) with a preload of  $\sim 3.6$  N/cm<sup>2</sup>. The shear strength, however, is drastically enhanced by the application of the parylene shell, with a maximum shear strength of  $\sim 38$  N/cm<sup>2</sup> obtained for  $t_p = 50$  nm and a preload of  $\sim 3.6$  N/cm<sup>2</sup>. This significant enhancement in the shear adhesion is attributed to the higher surface compliance of the parylene shell on the hard Ge NWs, enabling conformal contact with increased contact area between the interpenetrating NWs. This effect is clearly evident from the contact area calculations<sup>21</sup> between two parallel NWs based on the Hertz contact<sup>22</sup> for hard, pristine GeNWs and Johnson–Kendall–Roberts mechanics<sup>23</sup> for parylene-coated Ge NWs, indicating a contact width enhancement of  $\sim 115\times$  for  $t_p = 50$  nm as compared to the pristine Ge NWs (Figure 3d, see Supporting Information for detailed calculations).

A decrease in the shear adhesion of NW connectors is observed for  $t_p > 50$  nm. This trend is attributed to the higher

stiffness for thicker parylene shells, which reduces the conformal side contact between the interpenetrating NWs. Specifically, the  $t_p = 400$  nm NWs are calculated to have a bending stiffness  $\sim 1500$  times that of the  $t_p = 50$  nm NWs (Figure 3d). Additionally, the filling factor is increased for thicker parylene shells, which further reduces the NW interpenetration and the effective contact area. This hypothesis is directly confirmed by the microscale indentation tests, in which indentation depths of  $\sim 26$  and  $11$   $\mu\text{m}$  are observed for  $t_p = 50$  and  $200$  nm, respectively (see Figure S2 in Supporting Information). To examine the effect of miniaturization on the binding properties of the NW chemical connectors, microscopic shear adhesion tests were performed. Similar binding properties were observed for microscopic tests (area = 1–5 mm<sup>2</sup>), further confirming the generic characteristics of the NW connectors, independent of the connector size (see Figure S3 in Supporting Information). It should be noted that besides the shell thickness, the interpenetration depth of the NW connectors is expected to also depend on the NW length, especially since longer NWs tend to bend and collapse more readily. In the future, detailed studies of the geometric effects of the NW forests on the binding characteristics are needed to further optimize the connectors.

NW chemical connectors are highly nonsticky to foreign surfaces. As depicted in Figure 3a, the shear adhesion of NW connectors is strong for self-similar surfaces (i.e., surfaces with comparable geometric configuration to enable NW interpenetration) but weak on flat surfaces. For instance, NW forests with  $t_p = 200$  and  $400$  nm, exhibit minimal ( $< 0.8$  N/cm<sup>2</sup>) shear or normal adhesion on flat surfaces (i.e., glass



and parylene coated glass). This *self-selective* adhesion property arises from the drastically enhanced contact area (>25 times enhancement, see Supporting Information for detailed calculations) and intimate contact for the interpenetrating NW configuration as compared to that of NWs on flat surfaces (see Figure S2b in Supporting Information). This is highly attractive for connector applications where specific binding of the two components are desired, for instance, for reconfigurable structures (see Figure S4 in Supporting Information for a proof of concept demonstration), and presents a major contrast to the gecko adhesives which are highly sticky to most surfaces. As compared to the widely explored gecko-inspired adhesives which utilize carbon nanotube or polymeric fibrillar structures, the NW connectors have higher stiffness, especially for thick parylene shells, which reduces their contact area on flat surfaces.

Besides the parylene shell thickness, the shear adhesion strength is also affected by the preload force applied to engage the connectors. In general, a monotonic increase in the adhesion force is observed with the preload force (Figure 3b). Specifically, when the preload force is increased from 0.8 to 3.6 N/cm<sup>2</sup>, an enhancement of ~2 times in the shear adhesion strength is observed for  $t_p = 50$  nm, with the sensitivity of the adhesion strength decreasing for higher preloads (Figure 3b), and eventually reaching ~163 N/cm<sup>2</sup> for hand-engaged (preload ~100 N/cm<sup>2</sup>) binding tests (Figure 2a). This behavior is expected since the higher preload force results in an enhanced contact area between the NWs by increasing the extent of the interpenetration. It is also worth noting that an adhesion coefficient (shear to preload ratio) of ~24 is obtained for a preload force of 0.8 N/cm<sup>2</sup> (Figure 3a), which is significantly higher than most gecko-inspired adhesives.<sup>8,9,20,24,25</sup> Since the adhesion coefficient represents the efficiency of binding with respect to the applied force, NW connectors are highly useful for assembly processes requiring minimal engagement energy between the components.

As depicted in Figure 3b,c, NW connectors exhibit significantly higher shear than normal strength, which is a desirable property for connector applications requiring reusability with easy detachment. Specifically, shear to normal adhesion ratios of ~27 and 7 are obtained for a preload force of 2.8 and 30 N/cm<sup>2</sup>, respectively. This anisotropic adhesion behavior is due to the enhanced side contact between the interpenetrating NWs under a shear force. A shear force induces NW alignment in the shear direction (Figure 2a and see Figure S5 in Supporting Information), providing a higher probability of side contact between parallel NWs. Depending on the applied preload force (i.e., interpenetration depth), there seems to be two different shear failure modes, that is, interfacial and cohesive failure (see Figure S6 in Supporting Information). When the interpenetration depth is small, the interfacial vdW interaction is the limiting factor in determining the adhesion strength. However, beyond a critical interpenetration depth, the interfacial vdW interactions are strong enough to induce polymer necking and rupture of the hybrid NWs (see Figure S7 in Supporting Information), resulting in cohesive failure. Interestingly, within the inter-

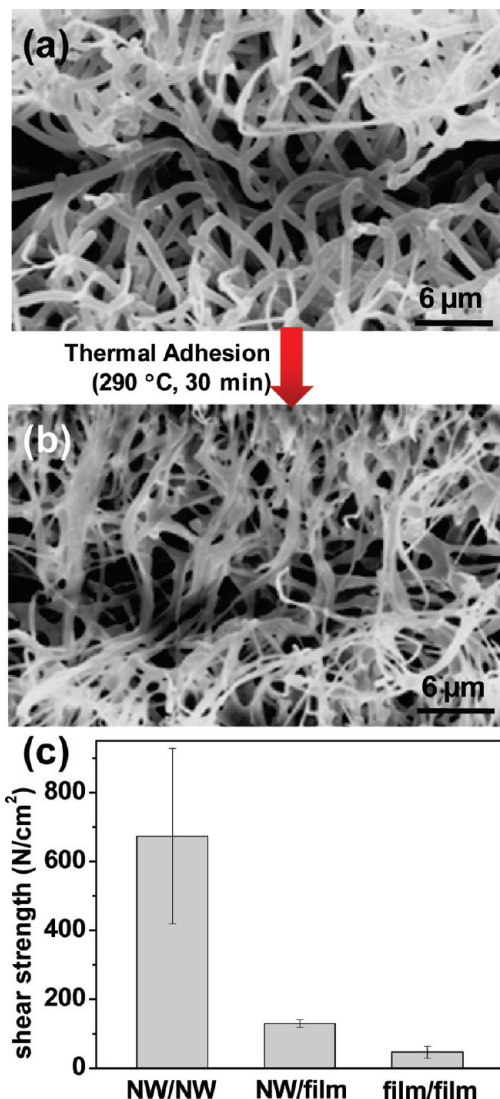


**Figure 4.** Permanent, thermal adhesion of NW connectors. Cross-sectional SEM images of interpenetrating NWs (a) before and (b) after the thermal adhesion at 290 °C for 30 min. (c) Comparison of the shear adhesion strength for NW/NW, NW/parylene film, and parylene film/parylene film after thermal adhesion at 290 °C for 30 min.

facial failure mode, NW connectors show reusability up to 27 times for an applied shear force of 1.2 N/cm<sup>2</sup> and a preload force of 0.8 N/cm<sup>2</sup> (see Figure S8 in Supporting Information). This reusability may be further enhanced in the future through materials optimization.

Besides vdW interactions, mechanical interlocking of the NWs, similar to those used in the hook and loop fasteners, may also affect the adhesion properties. In fact, the mechanical entanglement is evident from SEM images of the engaged NW connectors (Figure 2b,c). However, since the shear strength is significantly higher than the normal strength, we speculate that the mechanical interactions are not the dominant binding mechanism as such interactions are typically isotropic. Additionally, we find that when the surface of Ge/parylene NWs is hardened with enhanced surface roughness, for instance by depositing an ultrathin layer of Ti/Au (2/3 nm), a drastic decrease in the shear strength is

observed (see Figure S9 in Supporting Information). This result is indicative of the dominant role of the vdW interactions in NW connectors for which an intimate contact is essential.

Another unique feature of the hybrid NW connectors is their ability to controllably operate in either a reusable or permanent binding mode. The permanent binding mode is achieved through a thermal treatment of the engaged connectors during which the organic shell is melted, resulting in the bonding of the interpenetrating inorganic NWs from the two components (Figure 4a,b). The average observed shear strength of NW connectors after thermal adhesion at 290 °C (melting temperature of parylene-C used as organic shell) for 30 min is  $\sim 670$  N/cm<sup>2</sup> with a maximum value of  $\sim 980$  N/cm<sup>2</sup>. This impressive shear adhesion strength is comparable to that of most instant adhesives (414–2000 N/cm<sup>2</sup>, 3 M Scotch-Weld instant adhesives)<sup>26</sup> which shows the versatility of the hybrid NW forests as tunable connectors. Notably, the thermal adhesion for the interpenetrating NW connectors is well above the thermal adhesions obtained for planar parylene films ( $\sim 50$  N/cm<sup>2</sup>) as depicted in Figure 4c, demonstrating the importance of the fibrillar geometry and inorganic components of the interpenetrating NWs in gaining high permanent binding strength.

In conclusion, highly versatile *chemical* connectors that utilize nanoscale surface chemical binding interactions are reported and characterized in depth. The connectors are unisex and consist of interpenetrating, inorganic/organic core/shell NW forests with the inorganic core serving as the backbone and the organic shell providing the strength and the surface compliance needed to enable large contact areas. Because of the weak vdW bond strengths, the relatively stiff hybrid NW forests are highly nonsticky to nonsimilar foreign surfaces. However, the vdW interactions are drastically amplified when the high aspect ratio NW forests are engaged with self-similar surfaces, resulting in large contact area between the interpenetrating NW components, with the maximum shear strength approaching  $\sim 163$  N/cm<sup>2</sup>. The NW stiffness and surface compliance are directly tuned by the thickness of the parylene shell, therefore enabling a high degree of control for both the specific binding and the shear strength.

**Acknowledgment.** We thank J. C. Ho and Z. Zhang for useful discussions and technical help. This work was supported by DARPA/DSO, NSF, and Berkeley Sensor and Actuator Center. The nanowire synthesis part of this project was supported by a Laboratory Directed Research and Development grant from Lawrence Berkeley National Laboratory.

**Supporting Information Available:** Descriptions of the nanowire growth, parylene coating, and macroscopic and microscopic adhesion tests, calculations of contact area and bending stiffness, and additional figures showing images of NWs and hybrid NWs, indentation tests, connector characterization, modeled shear strength, and resuability tests. This material is available free of charge via the Internet at <http://pubs.acs.org>.

## References

- (1) Yim, M.; Zhang, Y.; Roufas, K.; Duff, D.; Eldershaw, C. *IEEE/ASME Trans. Mechatron.* **2002**, *7*, 442.
- (2) Cohn, M. B.; Böhringer, K. F.; Noworolski, J. M.; Singh, A.; Keller, C. G.; Goldberg, K. Y.; Howe, R. T. *Proc. SPIE* **1998**, *3511*, 2.
- (3) Baglio, S.; Castorina, S.; Savalli, N. *Scaling Issues and Design of MEMS*; John Wiley & Sons: Hoboken, NJ 2007.
- (4) Whitney, D. E. *J. Dyn. Syst., Meas., Control* **1982**, *104*, 65.
- (5) Arzt, E.; Gorb, S.; Spolenak, R. *Proc. Natl Acad. Sci. U.S.A.* **2003**, *100*, 10603.
- (6) Murphy, M.; Aksak, B.; Sitti, M. *J. Adhes. Sci. Technol.* **2007**, *21*, 1281.
- (7) Zhao, Y.; Tong, T.; Delzeit, L.; Kashani, A.; Meyyappan, M.; Majumdar, A. *J. Vac. Sci. Technol., B* **2006**, *24*, 331.
- (8) Qu, L.; Dai, L. *Adv. Mater.* **2007**, *19*, 3844.
- (9) Ge, L.; Sethi, S.; Ci, L.; Ajayan, P. M.; Dhinojwala, A. *Proc. Natl Acad. Sci. U.S.A.* **2007**, *104*, 10792.
- (10) Lee, J.; Fearing, R. S.; Komvopolous, K. *Appl. Phys. Lett.* **2008**, *93*, 191910.
- (11) Autumn, K.; Liang, Y. A.; Hsieh, S. T.; Zesch, W.; Chan, W.-P.; Kenny, W. T.; Fearing, R.; Full, R. J. *Nature* **2000**, *405*, 681.
- (12) Mrksich, M.; Whitesides, G. M. *Annu. Rev. Biophys. Biomol. Struct.* **1996**, *25*, 55.
- (13) Lieber, C. M.; Wang, Z. L. *MRS Bull.* **2007**, *32*, 99.
- (14) Xia, Y.; Yang, P.; Sun, Y.; Wu, Y.; Mayers, B.; Gates, B.; Yin, Y.; Kim, F.; Yan, H. *Adv. Mater.* **2003**, *15*, 353.
- (15) Ngo, L. T.; Alméjida, D.; Sader, J. E.; Daly, B.; Petkov, N.; Holmes, J. D.; Erts, D.; Boland, J. J. *Nano Lett.* **2006**, *6*, 2964.
- (16) Autumn, K. *MRS Bull.* **2007**, *32*, 473.
- (17) Thostenson, E. T.; Li, C.; Chou, T.-W. *Compos. Sci. Technol.* **2005**, *65*, 491.
- (18) Fortin, J. B.; Lu, T.-M. *Chemical Vapor Deposition Polymerization: The Growth and Properties of Parylene Thin Films*; Kluwer Academic: Norwell, MA 2004.
- (19) [www.torstamp.com/Brochures/BR-122.pdf](http://www.torstamp.com/Brochures/BR-122.pdf).
- (20) Qu, L.; Dai, L.; Stone, M.; Xia, Z.; Wang, Z. L. *Science* **2008**, *322*, 238.
- (21) Chaudhury, M. K.; Weaver, T.; Hui, C. Y.; Kramer, E. J. *J. Appl. Phys.* **1996**, *80*, 30.
- (22) Hertz, H. *J. Reine Angew. Math.* **1881**, *92*, 156.
- (23) Johnson, K. L.; Kendall, K.; Roberts, A. D. *Proc. R. Soc. London, Ser. A.* **1971**, *324*, 301.
- (24) Kustandi, T. S.; Samper, V. D.; Yi, D. K.; Ng, W. S.; Neuzil, P.; Sun, W. X. *Adv. Funct. Mater.* **2007**, *17*, 2211.
- (25) Geim, A. K.; Dubonos, S. V.; Grigorieva, I. V.; Novoselov, K. S.; Zhukov, A. A.; Shapoval, S. Yu. *Nat. Mater.* **2003**, *2*, 461.
- (26) [www.3m.com/sg-iatd/products/pdf/structural\\_adhesives/3M\\_Scotch\\_Weld\\_Epoxy\\_Instant\\_Adhesives.pdf](http://www.3m.com/sg-iatd/products/pdf/structural_adhesives/3M_Scotch_Weld_Epoxy_Instant_Adhesives.pdf).

NL900343B